Water-Soluble Polyelectrolyte-Grafted Multiwalled Carbon Nanotube Thin Films for Efficient Counter Electrode of Dye-Sensitized Solar Cells

Jinkyu Han, Hyunju Kim, Dong Young Kim, Seong Mu Jo, and Sung-Yeon Jang*

Polymer Hybrids Center, Korea Institute of Science and Technology, 39-1 Hawolgok-dong, Sungbuk, Seoul 136-791, Korea

D ye-sensitized solar cells (DSSCs) have attracted considerable attention as one of the next generation solar cells owing to their simple process and relatively high energy conversion efficiency at reasonable cost.[1] The panchromatic photoabsorption of dyes, rapid electron transfer at high surface area photoanodes, good ion transporting electrolytes, and efficient reduction of redox media at the counter electrodes (CEs) are the crucial components that determine the power conversion efficiency (PCE) of DSSCs. During photoelectrochemical generation, the redox species that are used as a mediator for regenerating the excited state dyes are reduced at the CE. Hence, the electrochemical catalytic activity for reduction, high surface area, and sufficient electrical conductivity are the essential properties for a good CE. Platinum-loaded transparent conducting electrodes (TCOs) prepared by sputtering, electrochemical deposition, or thermal reduction have excellent electrochemical catalytic activity as CEs.[2−4] However, the high cost and risk of Pt corrosion by the redox species in the electrolyte[5] have highlighted the need for low-cost, easily scalable, and more corrosion stable materials for CEs.

Carbon-based materials have recently attracted attention as practical materials for CE in DSSCs (DSSC-CE) because of their low cost, good electrochemical catalytic activity, and chemical stability. A high surface area, which is a preferred property for a DSSC-CE, could be obtained by controlling the size and morphology, and the surface characteristics could be manipulated by chemical means.[6,7] Furthermore, they are quite stable in a typical electrolyte system for DSSCs containing redox species. Several

ABSTRACT Water-soluble, polyelectrolyte-grafted multiwalled carbon nanotubes (MWCNTs), MWCNT-g-PSSNa, were synthesized using a "grafting to" route. MWCNT-g-PSSNa thin films fabricated by an electrostatic spray (e-spray) technique were used as the counter electrode (CE) for dye-sensitized solar cells (DSSCs). The e-sprayed MWCNT-g-PSSNa thin-film-based CEs (MWCNT-CE) were uniform over a large area, and the well-exfoliated MWCNTs formed highly interconnected network structures. The electrochemical catalytic activity of the MWCNT-CE at different thicknesses was investigated. The MWCNT-g-PSSNa thin film showed high efficiency as a CE in DSSCs. The power conversion efficiency (PCE) of the DSSCs using the MWCNT-g-PSSNa thin-film-based CE (DSSC-MWCNT) was >6% at a CE film thickness of ~0.3 μm. The optimum PCE was >7% at a film thickness of ~1 μm, which is 20−50 times thinner than conventional carbon-based CE. The charge transfer resistance at the MWCNT-CE/electrolyte interface was 1.52 Ω cm² at a MWCNT-CE thickness of 0.31 μm, which is lower than that of a Pt-CE/electrolyte interface, 1.78 Ω cm². This highlights the potential for the low-cost CE fabrication of DSSCs using a facile deposition technique from an environmentally "friendly" solution at low temperatures.

KEYWORDS: carbon nanotubes · water-soluble carbon nanotubes · dye-sensitized solar cell · electrospray · counter electrode

different carbon-based materials, such as active carbon,[8] carbon powder,[9,10] hard carbon sphere,[11] carbon nanotubes,[12] and fullerenes,[13] have been used as CEs exhibiting reasonable performance. The resulting PCEs of DSSCs using carbon-based CEs are slightly lower than those of DSSCs using Pt-based CEs. The high electrical conductivity[14] and electrochemical catalytic effect[15,16] of carbon nanotubes (CNTs) have been well-documented, and their application to DSSC-CE has been reported.[12,17] In CNTs, exfoliation and dispersion in solution are the key issues for optimizing their electrical and electrochemical properties as well as the processing capability because the bundling of CNTs reduces the surface area and alters the electrical properties of CNTs. A range of techniques to obtain well-exfoliated stable dispersions of CNT solutions have been studied extensively with functionalization *via* covalent and noncovalent routes being the major strategies.[18−20]
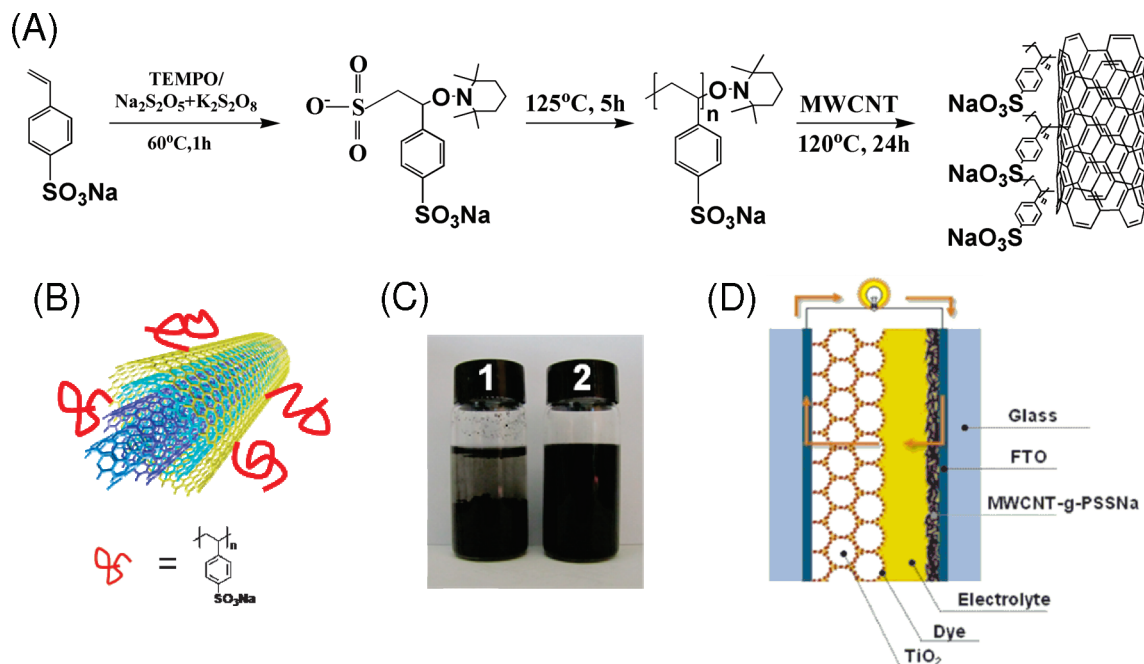
Figure 1. (A) Synthetic scheme of MWCNT-g-PSSNa, (B) structure of MWCNT-g-PSSNa, (C) photo images of pristine MWCNT, **1**, and MWCNT-g-PSSNa, **2**, in DI water, (D) schematic diagram of dye-sensitized solar cells. The concentration of both solutions was 1.25 mg mL^{-1}.

Highly processable CNT solutions, a facile deposition method to obtain uniform films, and well-exfoliated and interconnected network structures of individual CNTs with high electrochemical catalytic activity are essential for the reliable fabrication of CNT-based high-performance DSSC-CEs. In this study, water-soluble MWCNTs with polyelectrolytes attached covalently were synthesized for CNT-based DSSC-CEs. Uniform films of poly(styrene-4-sodiumsulfonate) (PSSNa) grafted MWCNT (MWCNT-g-PSSNa) were prepared from its aqueous solutions using an electrostatic spray (e-spray) method. The DSSCs were fabricated using the e-sprayed MWCNT-g-PSSNa thin films on FTO/glass, as CEs (MWCNT-CE), and their J−V characteristics and electrochemical catalytic effect with respect to the MWCNT-CE film thickness were investigated. The electrical properties of the MWCNT-g-PSSNa thin films were also measured. The PCE of the water-soluble MWCNT-based DSSCs (DSSC-MWCNT) was >6% at a CE film thickness of ∼0.3 μm, where the charge transfer resistance (R_{CT}) at the MWCNT-CE/electrolyte interface was optimized. The highest PCE of the DSSC using these water-processable MWCNT thin films as a CE was 7.03%, which is comparable to that of high-performance DSSCs using efficient Pt-based CEs (Pt-CE).

RESULTS AND DISCUSSION

Figure 1 shows the synthetic scheme and structure of the MWCNT-g-PSSNa, a polyelectrolyte-grafted MWCNT, which was synthesized using the "grafting to" route.[21] Briefly, 2,2,6,6-tetramethylpiperidinyl-1-oxyl (TEMPO)-terminated PSSNa (PSSNa-TEMPO) was first synthesized by nitroxide-mediated radical polymeriza-

tion using redox-type initiators.[22,23] The controlled length of the PSSNa-TEMPO having number averaged molecular weight (M_n) of 16 000 g mol^{-1} (PDI = 1.38), determined by gel permeation chromatography (GPC) using PSSNa as a standard, was obtained. The PSSNa-TEMPO was then reacted with MWCNT in ethylene glycol at 130 °C for 24 h to yield the PSSNa-grafted MWCNT, as shown in Figure 1. Upon heating at 130 °C, homolytic bond cleavage between TEMPO and PSSNa yielded radical-ended PSSNa that could react with the edge and/or side walls of the MWCNTs.[24,25] PSSNa is a nontoxic water-soluble polymer with higher thermal stability (melting point is 460 °C) due to its ionic interaction. It has been used as a dispersant in aqueous media for highly insoluble materials, such as graphene nanoplatelets and poly(3,4-ethylenedioxythiophene) (PEDOT).[26,27] The grafted PSSNa chains on the MWCNT enhance the solubility in many polar solvents, such as DMF, NMP, ethanol, and water dramatically. As shown in Figure 1C 1.25 mg mL^{-1} of the MWCNT-g-PSSNa could be dissolved in deionized (DI) water, whereas the pristine MWCNTs were insoluble. The weight fraction of the PSSNa on the MWCNT was approximately 6%, as determined by elemental analysis (data not shown) and thermogravimetric analysis (TGA) (see Figure S1 in Supporting Information).

MWCNT-g-PSSNa thin films were fabricated using an e-spray technique. E-spray deposition is a practical process that can deposit thin films of a variety of materials, such as polymers,[28,29] biomaterials,[30,31] inorganics,[32−34] and CNTs,[35] on a range of substrates. The e-spray method has the following advantages: (i) the film thickness, morphology, and uniformity can be
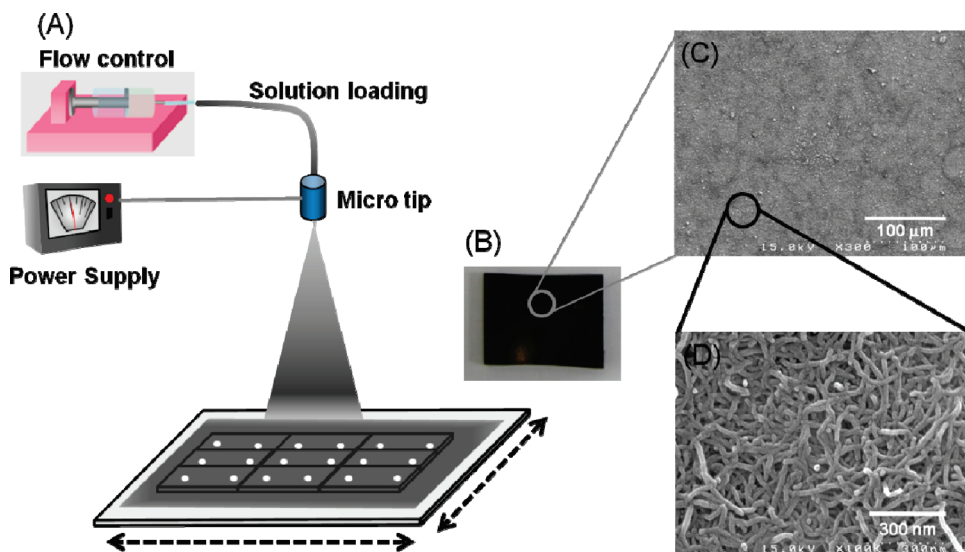
Figure 2. (A) Schematic diagram of the e-spray technique used for MWCNT-g-PSSNa thin film fabrication. (B) Photo image of e-sprayed MWCNT-g-PSSNa thin film (~1 μm thick). SEM images of e-spayed MWNT-g-PSSNa film on FTO/glass substrate at low magnification (×300) (C), and high magnification (×100 000) (B).

controlled easily by manipulating the concentration and injection flow rate of the e-spraying solution; (ii) the apparatus of the technique is simple; and (iii) it is a room temperature procedure.[35] Figure 2A shows a schematic diagram of the e-spray method used in this study. In principle, an aqueous solution of MWCNT-g-PSSNa was injected into a spraying capillary at a constant flow rate (~30 mL min^{-1}). Under high voltage application (>15 kV), the electric field overcomes the surface tension of the droplet, resulting in the atomization of numerous charged mists. Finally, the MWCNT-g-PSSNa films were deposited on fluorine-doped tin oxide (FTO)/glass. In the e-spray method, the mists are identically charged, which reduces agglomeration, and the collecting substrate is oppositely charged, which provides electrostatic adhesion that assists in even coverage.[36] This electrodynamic deposition mechanism is gentle and efficient, consuming a lower amount of material than other coating methods.[37] During e-spray deposition, the movable $x-y$ positioning stage was controlled to minimize undesired variations in the electric field that can cause thickness variations. It should be noted that all deposition processes were performed in the atmosphere at room temperature without heating the substrate, and no further sintering step was used because the resulting e-spray MWCNT-g-PSSNa films contains no binder. Figure 2B shows a photograph of e-sprayed MWCNT-g-PSSNa film (1 μm thick) deposited on the FTO/glass. The thicknesses of the e-sprayed films could be controlled easily from tens of nanometers to a few hundred micrometers by varying the solution concentration, flow rate, and/or e-spraying time. The films had a quite shiny appearance under typical room light, which indicates the uniformity and smoothness of the film surface. Figure 2C,D shows scanning electron microscopy (SEM) images of the e-sprayed

MWCNT-g-PSSNa films on FTO/glass. As shown in Figure 2C, the surface of the resulting film was uniform and showed no noticeable aggregation that is normally observed in poorly dispersed MWCNT films.[17] This suggests that the MWCNT-g-PSSNa solution combined with electrodynamic deposition technique limits CNT aggregation. The high-magnification SEM images in Figure 2D revealed the MWCNT-g-PSSNa film to consist of well-controlled interpenetrating network structures, where the connectivity of the electrical charge transport channels are well-preserved. The diameter and length of the MWCNT-g-PSSNa was ~15 nm and greater than a few micrometers, respectively. This well-exfoliated network morphology is essential for the good electrical conductivity and high surface area of the MWCNT-based films.

The electrical properties of the MWCNT-g-PSSNa films deposited on glass substrates were examined. Figure 3 shows the sheet resistance and electrical conductivity of the e-sprayed MWCNT-g-PSSNa films as a function of the film thickness. The thickness was determined
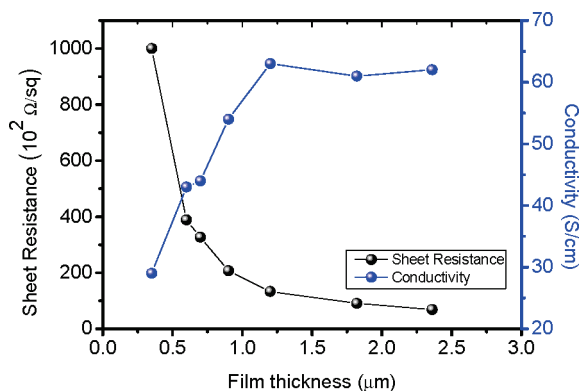

Figure 3. Sheet resistance and conductivity of MWCNT-g-PSSNa thin films on glass substrates as a function of the film thickness.
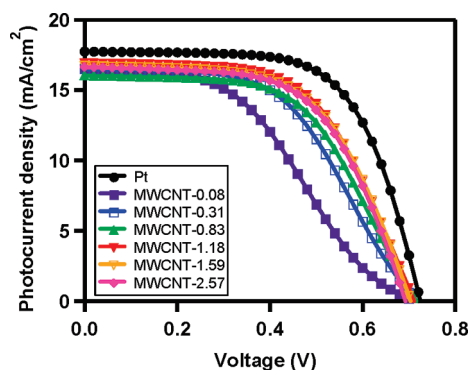
Figure 4. *J*−*V* characteristics of DSSC-MWCNTs at various CE thickness and a DSSC-Pt under simulated AM 1.5 light (● Pt, ■ 0.08 μm, □ 0.31 μm, ▲ 0.83 μm, ▼ 1.18 μm, ▽ 1.59 μm, ◆ 2.57 μm).

using a surface profiler (TENCOR P-10) and was controlled by the e-spraying time at flow rate of 30 mL min^{-1} using a 1 mg mL^{-1} MWCNT-g-PSSNa solution in DI water/ethanol (4/1). The electrical properties follow the typical behavior of other CNT-based films; that is, the sheet resistance decreases and the electrical conductivity increases with increasing film thickness. The enhancements in the electrical properties became saturated at a thickness ~1 μm, which is expected from the high-quality networked CNT films.[38] The saturated sheet resistance and electrical conductivity were 70 Ω/□ and 60 S/cm, respectively.

Inspired by the good electrical properties and uniform film morphology of the MWCNT-g-PSSNa thin films, we fabricated DSSCs using the e-sprayed MWCNT-g-PSSNa films as a CE (DSSC-MWCNT), and their performance was compared with that of Pt-CE-based DSSC (DSSC-Pt). In DSSC fabrication, doctor bladed TiO$_2$ nanoparticles (Nanoxide D, Solaronix) on FTO/glass followed by sintering at 500 °C for 30 min were used as photoanodes. The N719 sensitizer was loaded on the surface of the TiO$_2$ nanoparticles by immersing the photoanodes into a dilute ethanolic solution. The DSSCs were assembled and filled with the electrolyte system (details are in the Experimental Section). The Pt-CE was prepared by a thermal reduction method, which is known to have the highest Pt-CE performance.[2,39] Briefly, a Pt precursor solution was drop coated on FTO/glass followed by a thermal treatment at 400 °C to form highly crystalline Pt layers. Figure 4 shows the *J*−*V* characteristics of the DSSCs under 1 sun illumination (100 mW cm^{-2}, AM 1.5G). The PCE of the DSSC-MWCNTs improved with increasing CE thickness up to 1.18 μm and remained constant or decreased slightly with further increases in thickness (Table 1). The highest PCE for the DSSC-MWCNTs was 7.03% with an open circuit voltage (V_{OC}), short circuit current density (J_{SC}), and fill factor (FF) of 711 mV, 16.9 mA, and 58.5%, respectively. It should be noted that the PCE of DSSCs using a bare FTO/glass (without MWCNT) as a CE was <0.1%, indicating that FTO has negligible electrocatalytic activity.

TABLE 1. *J*−*V* Analysis Results of MWCNT-DSSCs at Different CE Thicknesses and a MWCNT-Pt

CE thickness (μm)	V_{OC} (V)	J_{SC} (mA/cm^2)	FF (%)	PCE (%)
Pt	0.724	17.74	64.6	8.30
0.08	0.710	16.54	41.9	4.90
0.31	0.713	16.49	52.3	6.15
0.83	0.716	16.02	56.1	6.43
1.18	0.711	16.90	58.5	7.03
1.59	0.703	16.70	58.9	6.91
2.57	0.692	16.63	59.3	6.82

The PCE enhancement was attributed mainly to the improved FF at thicker MWCNT-CE, while the V_{OC} and J_{SC} were relatively unaffected. In general, the FF of the DSSCs was related directly to the internal series resistance (R_S) of the DSSCs, which is composed of various components for photoelectrochemical generation.[40,41]

Electrochemical impedance spectroscopy (EIS) results provide useful information on the R_S of DSSCs, which helps further understand the relationship between the CE properties and resulting PCEs. Figure 5 shows the highest frequency regime of the Nyquist plot of the DSSC-MWCNTs and DSSC-Pt at open circuit condition under 1 sun illumination. In typical EIS analysis, the R_S of DSSCs is generally composed of at least three internal resistances.[40] The semicircles in the different frequency regimes indicate the Nernst diffusion-limited impedance of the redox species in the electrolyte, impedance by transport and recombination competition at the TiO$_2$/dye/electrolyte interface (R_{AN}), and electrochemical charge transfer resistance at the CE/electrolyte interface (R_{CT}).[40,42] The semicircle at the highest frequency regime in Figure 5 is related to the CE/electrolyte event, and the R_{CT} at the CE/electrolyte interface can be obtained from the real component (Z') values. Table 2 lists the R_{CT} of the DSSC-MWCNTs and DSSC-Pt. The optimized R_{CT} value of DSSC-MWCNT was ~1.2 Ω cm^2 at a thickness of 1.18 μm, which is similar to, or even lower than, that of the optimized DSSC-Pt, 1.78 Ω cm^2, indicating that the MWCNT-CE with a very
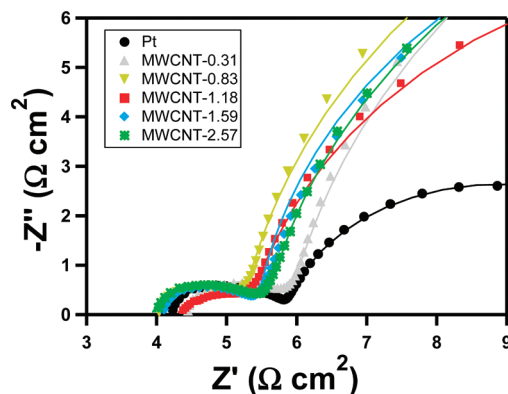

Figure 5. Nyquist plots of DSSC-MWCNTs at various CE thicknesses and a DSSC-Pt at the open circuit condition under simulated AM1.5 light (● Pt, ▲ 0.31 μm, ▼ 0.83 μm, ■ 1.18 μm, ◆ 1.59 μm, ■ 2.57 μm).

TABLE 2. Electrochemical Impedance Analysis Results of the MWCNT-DSSCs at Different CE Thicknesses and a Concurrent MWCNT-Pt

CE thickness (μm)	R_{SH} (cm²)	R_{CT} (cm²)	R_{AN} (cm²)
Pt	4.11	1.78	6.06
0.31	4.41	1.52	28.0
0.83	4.01	1.25	25.4
1.18	4.28	1.20	16.3
1.59	4.05	1.40	20.5
2.57	3.93	1.68	23.2

thin film has similar or even slightly better electrocatalytic activity that Pt-CE. The R_{CT} of DSSC-Pt was similar to the other values reported for high-performance Pt-CE-based DSSCs.[43] The sheet resistance (R_{SH}) of the DSSC-MWCNTs was relatively independent of the thickness of MWCNT-CE and comparable to the Pt-CE. This is because the CEs were prepared on the same FTO/glass, and the R_{SH} is dominated mainly by the electrical properties of the FTO/glass substrate when the deposition layers are thin enough.[41] The electrical conductivity of the MWCNT-g-PSSNa films and Pt layers prepared on FTO/glass was comparable (see Table S1 in Supporting Information).

The R_{CT} values of the DSSC-MWCNTs were slightly lower than that of DSSC-Pt, even at CE film thickness of 0.31 μm with a relatively weak thickness dependency. This is an important result compared to other reported carbon-based CE results, which are usually optimized using films tens of micrometers in thickness with strong thickness dependency.[8−10,44] To the best of our knowledge, the DSSC performance optimization at approximately 1 μm of CE thickness is by far the thinnest of the reported carbon-based CE results. Surprisingly, the PCE of DSSC-MWCNTs was >85% of the optimized value even when the CE thickness was decreased to 0.31 μm. Since FTO has negligible electrocatalytic activity, the weak thickness dependence of the MWCNT-CEs on the R_{CT} must be due to their intrinsic properties. The compact and uniform, yet well-networked, exfoliated morphology of our "binder-free" MWCNT thin films is believed to be responsible for the high electrochemical catalytic effect, possibly. The solubility and exfoliation of the MWCNT was leveraged by the Coulombic repulsion between the identically charged polyelectrolytes grafted on the MWCNTs.[26,27] The charge repulsion strategy has also been used to force the dispersion of highly rebuilding/restacking nanomaterials. For example, the chemical preparation of a stable aqueous dispersion of CNTs and graphite/graphene was achieved by enhancing the charge repulsion between them, which has become a very useful technique in nanocarbon chemistry.[45,46] The highly hydrophobic conjugated polymer, poly(3,4-ethlylenedioxy-thiophene) (PEDOT), was dispersed successfully in water by synthesizing in the presence of PSSNa to yield PEDOT-PSS, which is the most useful conducting polymer in organic electronic research. In addition to debundling by surface charge repulsion between MWCNT-g-PSSNa, the electrostatic attraction between the oppositely charged FTO/glass and MWCNT-g-PSSNa solution during e-spray deposition can enhance film deposition. The PCE of DSSC-MWCNT is comparable to that of the DSSC-Pt. The internal series resistance of the MWCNT-CEs was similar to or even lower than DSSC-Pt with a weak thickness dependency.[41]

CONCLUSIONS

Highly water-soluble, polyelectrolyte-grafted MWCNTs (MWCNT-g-PSSNa) were synthesized using a "grafting to" route. Thin films of the water-processable MWCNT-g-PSSNa were fabricated using an e-spray method without using any binder, and the resulting films were highly uniform over a large area maintaining an interconnected network structure of well-exfoliated MWCNTs due to the nature of the electrostatic charge-assisted deposition mechanism. The application of MWCNT-g-PSSNa thin films as a DSSC-CE had a comparable electrocatalytic effect to the Pt-CEs with slightly lower charge transfer resistance at the CE/electrolyte interface. The high PCE of DSSC-MWCNT could be obtained, even at the very thin CE film *ca.* 0.3 μm, and the PCE became comparable to that of the DSSC-Pt when the CE thickness was optimized to ~1 μm. This is 20−50 times thinner than the previously reported thickness of other carbon-based efficient CEs. This highlights the potential for the low-cost fabrication of Pt-free CE for DSSCs at low temperatures using a facile deposition technique in an environmentally "friendly" solvent.

EXPERIMENTAL SECTION

Materials: Sodium styrenesulfonate (SSNa), potassium persulfate, sodium metabisulfite, and 2,2,6,6-tetramethyl-1-piperidinyloxy (TEMPO) were purchased from Aldrich and used as received. MWCNTs (NC-7000) were obtained from Nanocyl and used after purification using the literature procedure.[47] The purity of MWCNT after purification determined by TGA was 98%. The sensitizer, *cis*-bis(isothiocyanato)bis(2,2′-bipyridyl-4,4′-dicarboxylato)ruthenium(II)bis-tetrabutylammonium (N719) was supplied by Solaronix SA and purified following a literature procedure prior to use.[48] 1-Butyl-3-methylimidazolium iodide (BMII),

iodine (I_2), 4-*tert*-butylpyridine (TBP), lithium iodide (LiI), acetonitrile (ACN), valeronitrile (VN), and dihydrogen hexachloroplatinate(IV) hexahydrate ($H_2PtCl_6 \cdot 6H_2O$) were used as received from Aldrich.

MWNT-g-PSSNa Synthesis: The MWCNT-g-PSSNa films were synthesized according to the methodology shown in Figure 1. TEMPO-terminated PSSNa was first prepared by a modification of the stable free radical polymerization (SFRP) process described by Keoshkerian *et al.*[22] and Bouix *et al.*[49] Briefly, SSNa (40 g, 194 mmol) and 2,2,6,6-tetramethyl-1-piperidinyloxy (2.96 g, 18.9 mmol) were dissolved in 200 mL of ethylene glycol (EG), and potassium persulfate (2.592 g, 9.6 mmol) in 45 mL of H_2O and so-

dium metabisulfite (1.368 g, 7.2 mmol) in 15 mL of H_2O were added to the solution at 130 °C under nitrogen. After 6 h, MWCNTs (0.4 g) were added to the solution and reacted for 24 h with vigorous stirring. A small amount of PSSNa was ejected through a syringe for characterization immediately before MWCNT addition. The solution was then cooled to room temperature, diluted in deionized water, and filtered repeatedly through a microporous cellulose membrane (0.22 μm) (three times). The MWCNT-g-PSSNa papers were isolated after drying the MWCNT-g-PSSNa covered filters overnight at room temperature under vacuum.

Preparation of MWCNT-CE and Pt-CE: Homogenously dispersed 0.1 wt % MWCNT-g-PSSNa in solutions of distilled water and ethanol (80/20, w/w) were obtained by ultrasonication for 30 min. The resulting solutions were deposited directly onto FTO/glass (TEC-8, Pilkington) using an e-spray technique. First, the MWCNT-g-PSSNa solution was loaded into a plastic syringe equipped with a 27-gauge stainless steel hypodermic needle. The needle was connected to a high voltage power supply (BERTAN SERIES 205B). A voltage of ~15 kV was applied between a metal orifice and the conducting substrate at a distance of 10 cm. The feed rate was controlled by the syringe pump (KD Scientific Model 220) at 25−30 μL min^{-1}. In order to form a uniform thickness over a large area, the nozzle and substrate were placed on a motion control system using a microprocessor. For comparison, a conventional Pt-CE was prepared by drop casting a 5 mM H_2PtCl_6 solution in isopropyl alcohol onto FTO/glass substrates followed by sintering at 400 °C for 20 min in air.

Fabrication of DSSC: A TiO_2 colloidal paste (Nanoxide-D, Solaronix) was doctor-bladed onto FTO/glass and sintered at 500 °C for 30 min in air. The resulting TiO_2 photoanode was immersed in an anhydrous ethanol solution containing 3×10^{-4} M of purified N719 dye and kept at room temperature for 24 h. The dye-adsorbed TiO_2 photoanode was assembled with MWCNT or platinum CE using a thermal adhesive film (24 μm thick Surlyn, Du-Pont) as a spacer to produce a sandwich-type cell. The liquid electrolyte consisting of 0.6 M 1-butyl-3-methylimidazolium iodide (BMII), 0.03 M iodine (I_2), 0.1 M lithium iodide (LiI), and 0.5 M 4-*tert*-butylpyridine (TBP) in a mixture of acetonitrile (ACN) and valeronitrile (VN) (85:15 v/v) was introduced through a drilled hole on the CEs. The holes were sealed with cover glass using Surlyn.

Characterization: The detailed morphology of the MWCNT-CEs was investigated using field emission scanning electron microscopy (FE-SEM, Hitachi S-4100). The electrical conductivity and sheet resistance were measured using microvolmeter (MCP-T610, Mitsubishi Chemical) in a four-probe setup at room temperature with a humidity of 35%. The photocurrent−voltage measurements were performed using a Keithley 2400 source measuring unit. A class A solar simulator (Newport, model 91195A-1000) equipped with a 450 W xenon lamp was used as a light source, and its light intensity was adjusted using a NREL-calibrated mono-Si solar cell equipped with a BF-7 filter to approximately AM 1.5 G, 1 sun light intensity. The electrochemical impedance spectra were measured using a frequency response analyzer (Solartron, SI 1260) connected to a potentiostat (Solartron 1287) at an amplitude of 10 mV at the open circuit voltage (V_{OC}) under 100 mW cm^{-2} illumination. The film thickness of the MWCNT-CE was determined using a surface profiler (P-10, Tencor). Thermogravimetric analysis (TGA) (TA Instruments) was performed under a flowing air atmosphere from 25 to 800 °C at a scan rate of 10 °C min^{-1}.

Supporting Information Available: Additional details for further analysis results. This material is available free of charge *via* the Internet at http://pubs.acs.org.

REFERENCES AND NOTES

1. Oregan, B.; Gratzel, M. A Low-Cost, High-Efficiency Solar-Cell Based on Dye-Sensitized Colloidal TiO_2 Films. *Nature* **1991**, *353*, 737–740.
2. Hauch, A.; Georg, A. Diffusion in the Electrolyte and Charge-Transfer Reaction at the Platinum Electrode in Dye-Sensitized Solar Cells. *Electrochim. Acta* **2001**, *46*, 3457–3466.
3. Gratzel, M. Conversion of Sunlight to Electric Power by Nanocrystalline Dye-Sensitized Solar Cells. *J. Photochem. Photobiol. A* **2004**, *168*, 235.
4. Nazeeruddin, M. K.; De Angelis, F.; Fantacci, S.; Selloni, A.; Viscardi, G.; Liska, P.; Ito, S.; Takeru, B.; Gratzel, M. G. Combined Experimental and DFT-TDDFT Computational Study of Photoelectrochemical Cell Ruthenium Sensitizers. *J. Am. Chem. Soc.* **2005**, *127*, 16835–16847.
5. Olsen, E.; Hagen, G.; Lindquist, S. E. Dissolution of Platinum in Methoxy Propionitrile Containing LiI/I$^{2−}$. *Sol. Energy Mater. Sol. Cells* **2000**, *63*, 267–273.
6. Xia, Y. D.; Walker, G. S.; Grant, D. M.; Mokaya, R. Hydrogen Storage in High Surface Area Carbons: Experimental Demonstration of the Effects of Nitrogen Doping. *J. Am. Chem. Soc.* **2009**, *131*, 16493–16499.
7. Benard, P.; Chahine, R. Determination of the Adsorption Isotherms of Hydrogen on Activated Carbons above the Critical Temperature of the Adsorbate over Wide Temperature and Pressure Ranges. *Langmuir* **2001**, *17*, 1950–1955.
8. Imoto, K.; Takahashi, K.; Yamaguchi, T.; Komura, T.; Nakamura, J.; Murata, K. High-Performance Carbon Counter Electrode for Dye-Sensitized Solar Cells. *Sol. Energy Mater. Sol. Cells* **2003**, *79*, 459–469.
9. Murakami, T. N.; Ito, S.; Wang, Q.; Nazeeruddin, M. K.; Bessho, T.; Cesar, I.; Liska, P.; Humphry-Baker, R.; Comte, P.; Pechy, P.; et al. Highly Efficient Dye-Sensitized Solar Cells Based on Carbon Black Counter Electrodes. *J. Electrochem. Soc.* **2006**, *153*, A2255–A2261.
10. Ramasamy, E.; Lee, W. J.; Lee, D. Y.; Song, J. S. Nanocarbon Counterelectrode for Dye Sensitized Solar Cells. *Appl. Phys. Lett.* **2007**, *90*, 173103.
11. Huang, Z.; Liu, X. H.; Li, K. X.; Li, D. M.; Luo, Y. H.; Li, H.; Song, W. B.; Chen, L. Q.; Meng, Q. B. Application of Carbon Materials as Counter Electrodes of Dye-Sensitized Solar Cells. *Electrochem. Commun.* **2007**, *9*, 596–598.
12. Suzuki, K.; Yamaguchi, M.; Kumagai, M.; Yanagida, S. Application of Carbon Nanotubes to Counter Electrodes of Dye-Sensitized Solar Cells. *Chem. Lett.* **2003**, *32*, 28–29.
13. Hino, T.; Ogawa, Y.; Kuramoto, N. Preparation of Functionalized and Non-functionalized Fullerene Thin Films on ITO Glasses and the Application to a Counter Electrode in a Dye-Sensitized Solar Cell. *Carbon* **2006**, *44*, 880–887.
14. Ebbesen, T. W.; Lezec, H. J.; Hiura, H.; Bennett, J. W.; Ghaemi, H. F.; Thio, T. Electrical Conductivity of Individual Carbon Nanotubes. *Nature* **1996**, *382*, 54–56.
15. Chew, S. Y.; Ng, S. H.; Wang, J. Z.; Novak, P.; Krumeich, F.; Chou, S. L.; Chen, J.; Liu, H. K. Flexible Free-Standing Carbon Nanotube Films for Model Lithium-Ion Batteries. *Carbon* **2009**, *47*, 2976–2983.
16. Chen, Y. S.; Huang, J. H.; Chuang, C. C. Glucose Biosensor Based on Multiwalled Carbon Nanotubes Grown Directly on Si. *Carbon* **2009**, *47*, 3106–3112.
17. Lee, W. J.; Ramasamy, E.; Lee, D. Y.; Song, J. S. Efficient Dye-Sensitized Cells with Catalytic Multiwall Carbon Nanotube Counter Electrodes. *ACS Appl. Mater. Interfaces* **2009**, *1*, 1145–1149.
18. Hirsch, A. Functionalization of Single-Walled Carbon Nanotubes. *Angew. Chem., Int. Ed.* **2002**, *41*, 1853–1859.
19. Petrov, P.; Stassin, F.; Pagnoulle, C.; Jerome, R. Noncovalent Functionalization of Multi-Walled Carbon Nanotubes by Pyrene Containing Polymers. *Chem. Commun.* **2003**, 2904–2905.
20. Sun, Y. P.; Fu, K. F.; Lin, Y.; Huang, W. J. Functionalized Carbon Nanotubes: Properties and Applications. *Acc. Chem. Res.* **2002**, *35*, 1096–1104.

21. Qin, S. H.; Qin, D. Q.; Ford, W. T.; Resasco, D. E.; Herrera, J. E. Functionalization of Single-Walled Carbon Nanotubes with Polystyrene *via* Grafting to and Grafting from Methods. *Macromolecules* **2004**, *37*, 752–757.

22. Keoshkerian, B.; Georges, M. K.; Boilsboissier, D. Living Free-Radical Aqueous Polymerization. *Macromolecules* **1995**, *28*, 6381–6382.

23. Ding, J. F.; Chuy, C.; Holdcroft, S. Enhanced Conductivity in Morphologically Controlled Proton Exchange Membranes: Synthesis of Macromonomers by SFRP and Their Incorporation into Graft Polymers. *Macromolecules* **2002**, *35*, 1348–1355.

24. Lou, X. D.; Detrembleur, C.; Pagnoulle, C.; Jerome, R.; Bocharova, V.; Kiriy, A.; Stamm, M. Surface Modification of Multiwalled Carbon Nanotubes by Poly(2-vinylpyridine): Dispersion, Selective Deposition, and Decoration of the Nanotubes. *Adv. Mater.* **2004**, *16*, 2123–2127.

25. Liu, Y. Q.; Yao, Z. L.; Adronov, A. Functionalization of Single-Walled Carbon Nanotubes with Well-Defined Polymers by Radical Coupling. *Macromolecules* **2005**, *38*, 1172–1179.

26. Stankovich, S.; Piner, R. D.; Chen, X. Q.; Wu, N. Q.; Nguyen, S. T.; Ruoff, R. S. Stable Aqueous Dispersions of Graphitic Nanoplatelets *via* the Reduction of Exfoliated Graphite Oxide in the Presence of Poly(sodium 4-styrenesulfonate). *J. Mater. Chem.* **2006**, *16*, 155–158.

27. Groenendaal, B. L.; Jonas, F.; Freitag, D.; Pielartzik, H.; Reynolds, J. R. Poly(3,4-ethylenedioxythiophene) and Its Derivatives: Past, Present, and Future. *Adv. Mater.* **2000**, *12*, 481–494.

28. Hoyer, B.; Sorensen, G.; Jensen, N.; Nielsen, D. B.; Larsen, B. Electrostatic Spraying: A Novel Technique for Preparation of Polymer Coatings on Electrodes. *Anal. Chem.* **1996**, *68*, 3840–3844.

29. Morozov, V. N.; Morozova, T. Y.; Kallenbach, N. R. Atomic Force Microscopy of Structures Produced by Electrospraying Polymer Solutions. *Int. J. Mass. Spectrom.* **1998**, *178*, 143–159.

30. Morozov, V. N.; Morozova, T. Y. Electrospray Deposition as a Method To Fabricate Functionally Active Protein Films. *Anal. Chem.* **1999**, *71*, 1415–1420.

31. Buchko, C. J.; Chen, L. C.; Shen, Y.; Martin, D. C. Processing and Microstructural Characterization of Porous Biocompatible Protein Polymer Thin Films. *Polymer* **1999**, *40*, 7397–7407.

32. Yu, Y.; Chen, C. H.; Shi, Y. A Tin-Based Amorphous Oxide Composite with a Porous, Spherical, Multideck-Cage Morphology as a Highly Reversible Anode Material for Lithium-Ion Batteries. *Adv. Mater.* **2007**, *19*, 993–997.

33. Chen, C. H.; Kelder, E. M.; vanderPut, P. J. J. M.; Schoonman, J. Morphology Control of Thin $LiCoO_2$ Films Fabricated Using the Electrostatic Spray Deposition (ESD) Technique. *J. Mater. Chem.* **1996**, *6*, 765–771.

34. Zhang, Y. Z.; Wu, L. H.; Xie, E. Q.; Duan, H. G.; Han, W. H.; Zhao, J. G. A Simple Method To Prepare Uniform-Size Nanoparticle TiO_2 Electrodes for Dye-Sensitized Solar Cells. *J. Power Sources* **2009**, *189*, 1256–1263.

35. Kim, J. H.; Nam, K. W.; Ma, S. B.; Kim, K. B. Fabrication and Electrochemical Properties of Carbon Nanotube Film Electrodes. *Carbon* **2006**, *44*, 1963–1968.

36. Jaworek, A. Electrospray Droplet Sources for Thin Film Deposition. *J. Mater. Sci.* **2007**, *42*, 266–297.

37. Rietveld, I. B.; Suganuma, N.; Kobayashi, K.; Yamada, H.; Matsushige, K. Electrospray Deposition of Photoresist: A Low Impact Method for the Fabrication of Multilayered Films. *Macromol. Mater. Eng.* **2008**, *293*, 387–399.

38. Lyons, P. E.; De, S.; Blighe, F.; Nicolosi, V.; Pereira, L. F. C.; Ferreira, M. S.; Coleman, J. N. The Relationship between Network Morphology and Conductivity in Nanotube Films. *J. Appl. Phys.* **2008**, *104*, 044302.

39. Murakami, T. N.; Gratzel, M.; Counter Electrodes for, D. S. C. Application of Functional Materials as Catalysts. *Inorg. Chim. Acta* **2008**, *361*, 572–580.

40. Han, L. Y.; Koide, N.; Chiba, Y.; Mitate, T. Modeling of an Equivalent Circuit for Dye-Sensitized Solar Cells. *Appl. Phys. Lett.* **2004**, *84*, 2433–2435.

41. Han, L. Y.; Koide, N.; Chiba, Y.; Islam, A.; Komiya, R.; Fuke, N.; Fukui, A.; Yamanaka, R. Improvement of Efficiency of Dye-Sensitized Solar Cells by Reduction of Internal Resistance. *Appl. Phys. Lett.* **2005**, *86*, 213501.

42. Fabregat-Santiago, F.; Bisquert, J.; Palomares, E.; Otero, L.; Kuang, D. B.; Zakeeruddin, S. M.; Gratzel, M. Correlation between Photovoltaic Performance and Impedance Spectroscopy of Dye-Sensitized Solar Cells Based on Ionic Liquids. *J. Phys. Chem. C* **2007**, *111*, 6550–6560.

43. Fang, X. M.; Ma, T. L.; Guan, G. Q.; Akiyama, M.; Kida, T.; Abe, E. Effect of the Thickness of the Pt Film Coated on a Counter Electrode on the Performance of a Dye-Sensitized Solar Cell. *J. Electroanal. Chem.* **2004**, *570*, 257–263.

44. Chen, J. K.; Li, K. X.; Luo, Y. H.; Guo, X. Z.; Li, D. M.; Deng, M. H.; Huang, S. Q.; Meng, Q. B. A Flexible Carbon Counter Electrode for Dye-Sensitized Solar Cells. *Carbon* **2009**, *47*, 2704–2708.

45. Liu, H.; Gao, J.; Xue, M. Q.; Zhu, N.; Zhang, M. N.; Cao, T. B. Processing of Graphene for Electrochemical Application: Noncovalently Functionalize Graphene Sheets with Water-Soluble Electroactive Methylene Green. *Langmuir* **2009**, *25*, 12006–12010.

46. Si, Y.; Samulski, E. T. Synthesis of Water Soluble Graphene. *Nano Lett.* **2008**, *8*, 1679–1682.

47. Wang; Shan, H.; Hauge, R. H.; Pasquali, M.; Smalley, R. E. A Highly Selective, One-Pot Purification Method for Single-Walled Carbon Nanotubes. *J. Phys. Chem. B* **2007**, *111*, 1249–1252.

48. Wang, Q.; Ito, S.; Gratzel, M.; Fabregat-Santiago, F.; Mora-Sero, I.; Bisquert, J.; Bessho, T.; Imai, H. Characteristics of High Efficiency Dye-Sensitized Solar Cells. *J. Phys. Chem. B* **2006**, *110*, 25210–25221.

49. Bouix, M.; Gouzi, J.; Charleux, B.; Vairon, J. P.; Guinot, P. Synthesis of Amphiphilic Polyelectrolyte Block Copolymers Using "Living" Radical Polymerization. Application as Stabilizers in Emulsion Polymerization. *Macromol. Rapid Commun.* **1998**, *19*, 209–213.

ARTICLE